JOURNAL OF GEOPHYSICAL RESEARCH, VOL. 112, D17303, doi:10.1029/2006JD007548, 2007

Transport of radon-222 and methyl iodide by deep convection in the GFDL Global Atmospheric Model AM2

Leo J. Donner,[1] Larry W. Horowitz,[1] Arlene M. Fiore,[1] Charles J. Seman,[1] Donald R. Blake,[2] and Nicola J. Blake[2]

Received 23 May 2006; revised 19 March 2007; accepted 10 July 2007; published 12 September 2007.

[1] Transport of radon-222 and methyl iodide by deep convection is analyzed in the Geophysical Fluid Dynamics Laboratory (GFDL) Atmospheric Model 2 (AM2) using two parameterizations for deep convection. One of these parameterizations represents deep convection as an ensemble of entraining plumes; the other represents deep convection as an ensemble of entraining plumes with associated mesoscale updrafts and downdrafts. Although precipitation patterns are generally similar in AM2 with both parameterizations, the deep convective mass fluxes are more than three times larger in the middle- to upper troposphere for the parameterization consisting only of entraining plumes, but do not extend across the tropopause, unlike the parameterization including mesoscale circulations. The differences in mass fluxes result mainly from a different partitioning between convective and stratiform precipitation; the parameterization including mesoscale circulations detrains considerably more water vapor in the middle troposphere and is associated with more stratiform rain. The distributions of both radon-222 and methyl iodide reflect the different mass fluxes. Relative to observations (limited by infrequent spatial and temporal sampling), AM2 tends to simulate lower concentrations of radon-222 and methyl iodide in the planetary boundary layer, producing a negative model bias through much of the troposphere, with both cumulus parameterizations. The shapes of the observed profiles suggest that the larger deep convective mass fluxes and associated transport in the parameterization lacking a mesoscale component are less realistic.

Citation: Donner, L. J., L. W. Horowitz, A. M. Fiore, C. J. Seman, D. R. Blake, and N. J. Blake (2007), Transport of radon-222 and methyl iodide by deep convection in the GFDL Global Atmospheric Model AM2, *J. Geophys. Res.*, *112*, D17303, doi:10.1029/2006JD007548.

1. Introduction

[2] Deep convection, characterized as it is by rapid motions between the planetary boundary layer (PBL) and middle and upper troposphere, plays a unique role in the vertical transport of surface emissions. Early tracer transport models treated this transport as enhanced diffusion, despite the clearly non-local character of deep convection. *Gidel* [1983] departed from these approaches by representing deep convection as an ensemble of entraining plumes, an approach consistent with the representation of the thermodynamic effects of deep convection that had been developed by *Arakawa and Schubert* [1974]. Unlike tracer profiles produced by representing deep convection as enhanced diffusion, *Gidel*'s [1983] entraining plumes generated increasing concentrations with height for some gases with surface sources. Subsequent studies have examined the role of convection in transporting particular species in chemical transport models and confirmed the behavior modeled by *Gidel* [1983]. *Feichter and Crutzen* [1990] and *Li and Chang* [1996] found that convection could play a dominant role in transporting radon-222 to the upper troposphere. *Allen et al.* [1996] and *Stockwell and Chipperfield* [1999] found that the extent of this transport was sufficiently large that C-shaped profiles of radon-222 were produced in their chemical transport models, with maxima for surface-source radon-222 both near the surface and in the upper troposphere. However, comparison with observations has suggested that these chemical transport models may convect too much tracer into the upper troposphere, as noted by *Stockwell and Chipperfield* [1999] and, for carbon monoxide, by *Allen et al.* [1997].

[3] The possibility that deep convection is important in the tracer budget of the stratosphere has been investigated using conceptual models [*Sherwood and Dessler*, 2003], cloud-resolving models [*Lu et al.*, 2000; *Mullendore et al.*, 2005], general circulation models (GCMs) [*Gray*, 2003], and observations [*Ridley et al.*, 2004; *Hegglin et al.*, 2004; *Ray et al.*, 2004]. The modeling studies have suggested multiple mechanisms for both upward and downward transport associated with convection around the tropopause, while the observational studies generally suggest convection plays a role in the stratospheric tracer budget, with

[1] Geophysical Fluid Dynamics Laboratory/NOAA, Princeton University, Princeton, New Jersey, USA.
[2] University of California, Irvine, California, USA.

0148-0227/07/2006JD007548$09.00

variation among reported cases as to whether convection directly injects tracers into the stratosphere.

[4] The locations and intensities of centers of deep convective activity change in association with interannual variability. *Gilliland and Hartley* [1998] and *Lintner et al.* [2004] have shown that interannual variability in the patterns of deep convection can induce changes in interhemispheric transport of tracers.

[5] Deep convection also affects the concentrations of aerosols and soluble gases through wet scavenging. For instance, *Liu et al.* [2001] and *Considine et al.* [2005] evaluated wet scavenging in their models using radionuclide tracers lead-210 (produced by radioactive decay of radon-222) and beryllium-7 (produced by cosmic ray spallation mostly in the stratosphere). *Liu et al.* [2001] found surface air observations of these species were sensitive to the magnitude of wet deposition. *Considine et al.* [2005] found that the relative magnitudes of convective transport and scavenging of lead-210 depended on the details of the chemical transport model and cumulus parameterization.

[6] In global chemical transport models and GCMs, the unresolved scale of deep convection requires its parameterization. Cumulus parameterizations remain plagued by fundamental uncertainties. *Mahowald et al.* [1995] and *Folkins et al.* [2006] found that these uncertainties propagate into the distribution of tracers transported by convection in global models. *Olivie et al.* [2004] computed mass fluxes with two different cumulus parameterizations, one interactively in a GCM and the other diagnostically with analyzed model fields, and noted differences in radon-222 and ozone distributions obtained using these mass fluxes in a chemical transport model. Using two cumulus parameterizations, rather than seven parameterizations, as had *Mahowald et al.* [1995], *Josse et al.* [2004] noted less dependence of tracer distribution on the method of parameterizing cumulus convection.

[7] These studies of convective transport of tracers indicate the importance of convection in determining tracer distributions in the troposphere and stratosphere, including their time-mean, interannual, and interhemispheric variability. The studies also suggest a dependence of these results on the method of parameterizing convection and a tendency for at least some parameterizations to transport excessively into the upper troposphere. The purpose of this paper is to examine tracer transport by a cumulus parameterization which explicitly includes two characteristics not present in the earlier studies and which may directly influence the extent of vertical transport and tracer injection into the stratosphere: mesoscale updrafts and downdrafts associated with deep convection. Extensive detrainment from deep convective cells occurs in the middle troposphere, and more of the latent heat release required to maintain atmospheric stability occurs in middle- and upper-tropospheric stratiform cloud systems than in a version of this parameterization with the mesoscale circulations inactive [*Donner et al.*, 2001]. Convective mass fluxes are consequently lower when mesoscale circulations are present, and, generally, this suggests excessive mass fluxes if mesoscale circulations are not parameterized as a part of convective systems. *Donner*'s [1993] parameterization also includes vertical velocities for the members of its cumulus ensemble, in contrast to earlier mass-flux methods. The vertical velocities are inferred by solving a momentum equation, which allows convective updrafts to overshoot their levels of zero buoyancy. Parameterizations based on mass fluxes without vertical velocities lack a basis for including this overshoot. Overshooting updrafts have the potential to change stratospheric tracer budgets relative to those whose tops are restricted to the level of zero buoyancy.

[8] We compare distributions of radon-222 and methyl iodide in two integrations of an atmospheric GCM, one using the *Donner* [1993] parameterization including mesoscale circulations and overshooting convective cells and the other using a parameterization which does not include them. Radon-222 has been used extensively in tracer studies in chemical transport models [*Feichter and Crutzen*, 1990; *Mahowald et al.*, 1997; *Stockwell et al.*, 1998; *Dentener et al.*, 1999; *Considine et al.*, 2005] and has a source that is fairly uniform over lower- and middle-latitude continents. By contrast, methyl iodide is emitted from marine areas, as well as from some sub-tropical and tropical continental regions, and provides a means of examining convection over oceanic areas [*Cohan et al.*, 1999; *Bell et al.*, 2002]. Both radon-222 and methyl iodide are insoluble and not subject to wet deposition; using them in this study places the focus on transport by convection. The paper will focus on vertical profiles during July (radon) and August through September (methyl iodide). These are periods when occurrence of deep convection over source regions is especially pronounced, with convective maxima in the Northern Hemisphere over continental radon sources and peak methyl iodide emissions around 20°N in the late northern summer. The parameterization which includes mesoscale circulations consistently detrains more radon and methyl iodide in the middle troposphere, and less in the upper troposphere, than the parameterization lacking these circulations, in better agreement with most observations. At the tropopause, the penetrative deep cells in the *Donner* [1993] parameterization can transport more radon and methyl iodide into the stratosphere than the parameterization based only on mass fluxes.

[9] Section 2 describes the GCM, cumulus parameterizations, and emissions. Section 3 examines the distributions of radon and methyl iodide and links differences between the GCM integrations to basic features of the cumulus parameterizations, and section 4 compares GCM results with observations.

2. GCM Configurations

[10] The atmospheric component AM2 of the Geophysical Fluid Dynamics Laboratory (GFDL) coupled climate model CM2 [*Delworth et al.*, 2006] is used for these tracer transport studies. Its finite-volume dynamical core [*Lin*, 2004] is used for large-scale advection of radon and methyl iodide, as is its sub-grid diffusion.

2.1. Cumulus Parameterizations

[11] Cumulus convection in AM2 is treated using a relaxed Arakawa-Schubert parameterization [*Moorthi and Suarez*, 1992] with modifications described in *GFDL Global Atmospheric Model Development Team* [2004]. This parameterization represents cumulus convection as an ensemble of entraining plumes characterized by mass fluxes.

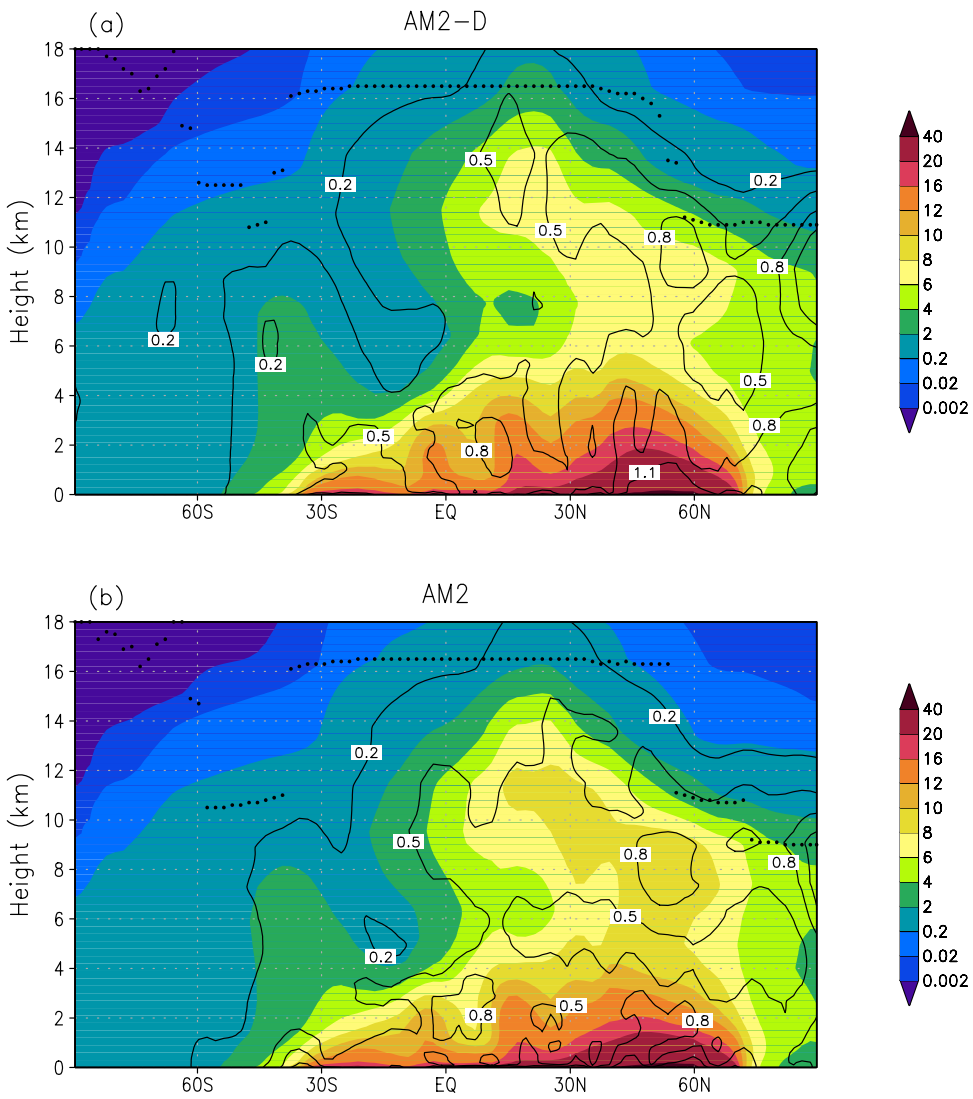

Figure 1. Zonal averages of volume mixing ratio for radon for July for (a) AM2-D and (b) AM2. Temperature minimum (as an indication of the tropopause) shown by dark circles. Solid lines indicate standard deviations of monthly means, with contour levels 0.2, 0.5, 0.8, and 1.1.

Since there is no representation of cumulus-scale vertical velocities, its convective microphysics is simple, consisting only of a fractional conversion of condensate to precipitation, with the remaining condensate detrained into stratiform clouds. No mesoscale circulations or convective downdrafts are included.

[12] Radon and methyl iodide transport in AM2 is contrasted in this paper with their transport in a version of AM2 using the cumulus parameterization of *Donner* [1993]; this version of the model is denoted as AM2-D. The implementation of this cumulus parameterization follows *Donner et al.* [2001], except that (1) *Zhang*'s [2002, 2003] closure is used and (2) *Wilcox and Donner*'s [2007] procedure is used to parameterize the ice contents in the mesoscale stratiform updrafts (anvils), which are part of deep convective systems. This cumulus parameterization provides the mass fluxes and vertical velocities for members of cumulus ensembles. The cumulus vertical velocities drive bulk microphysics and allow ensemble members to both overshoot and undershoot their levels of neutral buoyancy.

[13] Another distinctive aspect of this cumulus parameterization is its representation of mesoscale updrafts and downdrafts, characterized by both lateral transfers of water vapor and ice from the ensemble of cumulus cells and phase changes associated with mesoscale motions. The partitioning of mass flux among members of the ensemble of cumulus cells differs in the two parameterizations. In the relaxed Arakawa-Schubert parameterization, the mass flux for each ensemble member is chosen so that the effect of the ensemble member is to relax its cloud work function toward

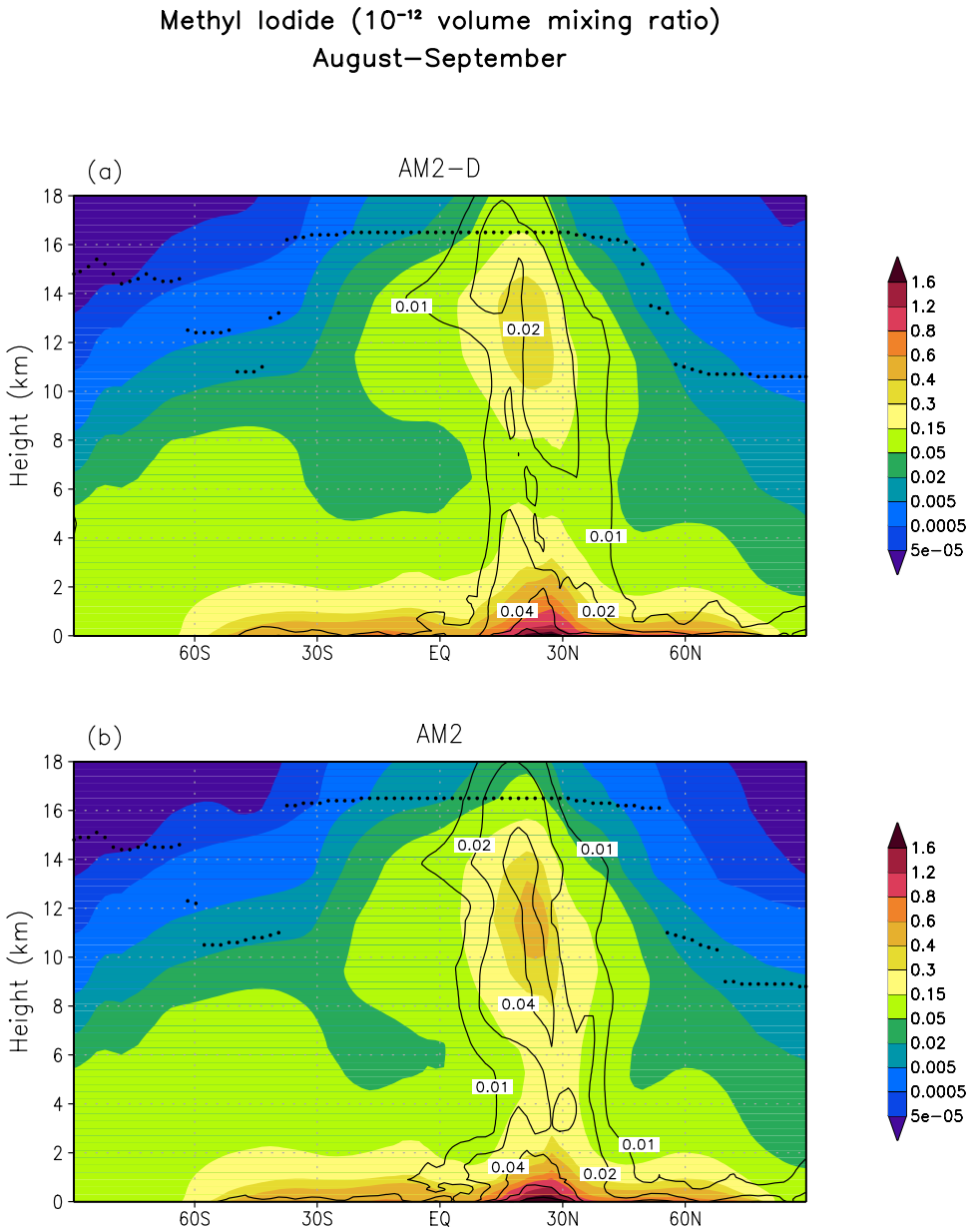

Figure 2. Zonal averages of volume mixing ratio for methyl iodide for August–September for (a) AM2-D and (b) AM2. Temperature minimum (as an indication of the tropopause) indicated by dark circles. Solid lines indicate standard deviations of August-September means, with contour levels 0.01, 0.02, 0.04, 0.06, and 0.10.

a critical value over a prescribed timescale. The cloud work function is the energy released by a parcel with a characteristic fractional entrainment rate as it ascends to its level of neutral buoyancy. For zero entrainment, cloud work function is convective available potential energy (CAPE). In the *Donner* [1993] parameterization, the mass flux is partitioned among ensemble members according to a distribution function of entrainment coefficients for the members, obtained from observations of deep convective vertical velocities and normalized by the total mass flux of the ensemble. The closure is then applied to the full convective system, consisting of both the cumulus cells and the mesoscale circulations. In general, the *Donner* [1993] ensemble detrains extensively in the middle troposphere, where its detrained water vapor and ice build the mesoscale anvil (updraft) circulation. In the absence of a mesoscale circulation in the relaxed Arakawa-Schubert parameterization, the ensemble members tend to detrain at greater heights. Since the *Donner* [1993] parameterization is designed to represent deep convection only, the relaxed Arakawa-Schubert parameterization is retained in AM2-D to represent shallow convection, by requiring that its cumulus ensembles have cloud tops at pressures of at least 500 hPa.

[14] The characteristics of the cumulus parameterizations in AM2 and AM2-D are summarized in the Appendix.

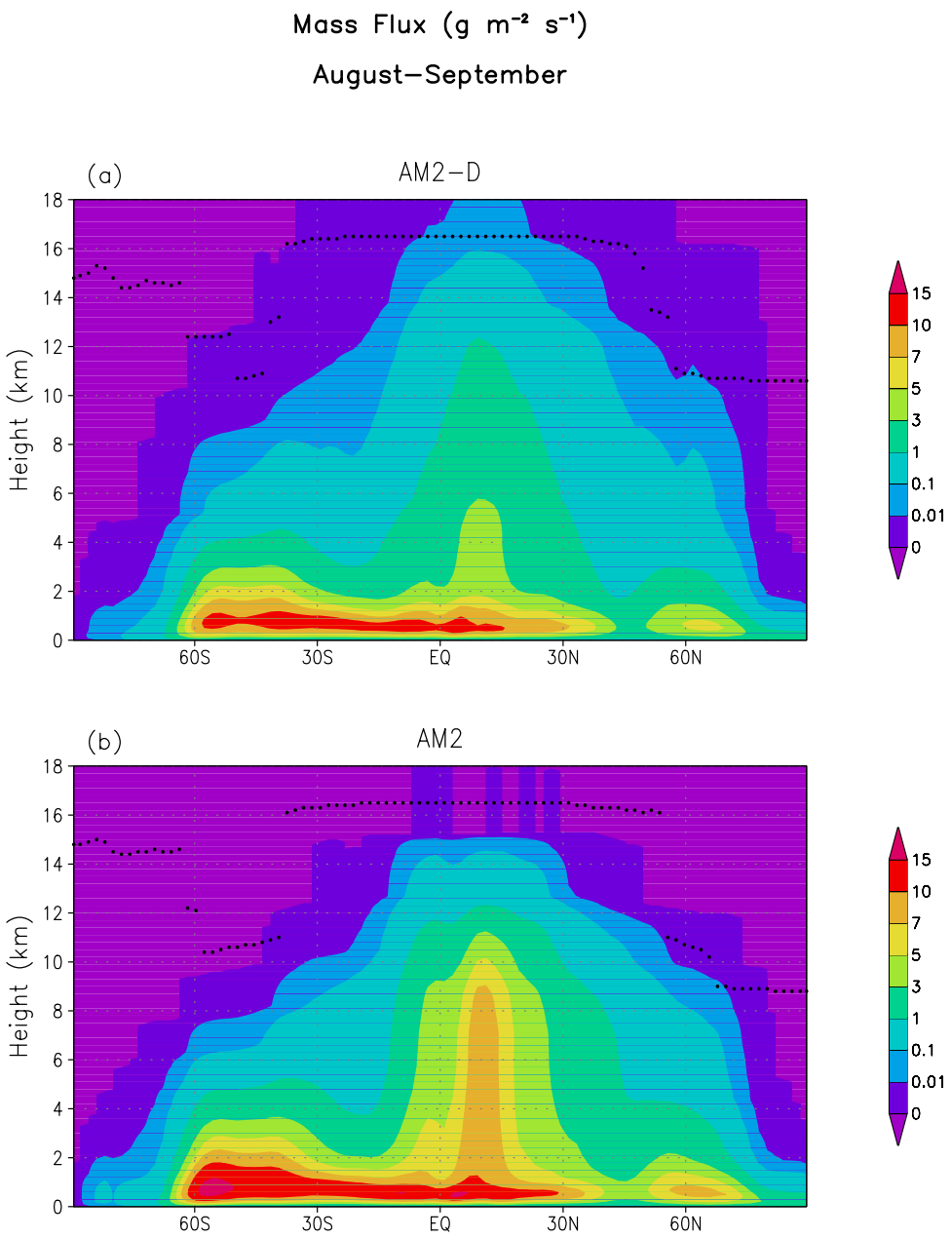

Figure 3. Zonal averages of cumulus mass fluxes for August–September for (a) AM2-D and (b) AM2. Temperature minimum (as an indication of the tropopause) indicated by dark circles.

2.2. Sources and Sinks

[15] Radon-222 is produced in soils from the radioactive decay of radium-226. While the emission rate of radon-222 to the atmosphere can vary locally depending on soil texture and radium-226 content, soil moisture, and soil freezing, there is little data to quantify such effects. Thus we adopt a simple representation of radon-222 emissions, similar to that commonly used in model studies (e.g., the model intercomparison study of *Jacob et al.* [1997]), in which an emission rate of 10^4 atoms m^{-2} s^{-1} is assumed from land at latitudes below 60°N, and a rate of half that amount from land between 60–70°N (except Greenland, where emissions are assumed to be zero). Weak emissions from oceans and other land areas are neglected in this study. Total radon emissions are 14.6 kg y^{-1}. Radon decays with an e-folding lifetime of 5.5 days. While uncertainty in dependence of radon emissions on soil characteristics precludes more detailed treatment in this study, we note that this may limit the realism of the results; *Chevillard et al.* [2002] found that allowing variations of a factor of five in radon emissions related to soil type was insufficient to produce good agreement between observed values of radon and those simulated at some locations by a regional model.

[16] Methyl iodide emissions are those of *Bell et al.* [2002] and total 3.05 × 10^8 kg y^{-1} and include emissions from oceans (2.14 × 10^8 kg y^{-1}), biomass burning (9.32 × 10^6 kg y^{-1}), biofuels (3.51 × 10^6 kg y^{-1}), wetlands (7.20 × 10^6 kg y^{-1}) and, prominently, rice paddies (7.10 × 10^7 kg y^{-1}). Methyl iodide undergoes photolysis during the daytime at a rate of 5.79 × 10^{-6} s^{-1}, corresponding to a

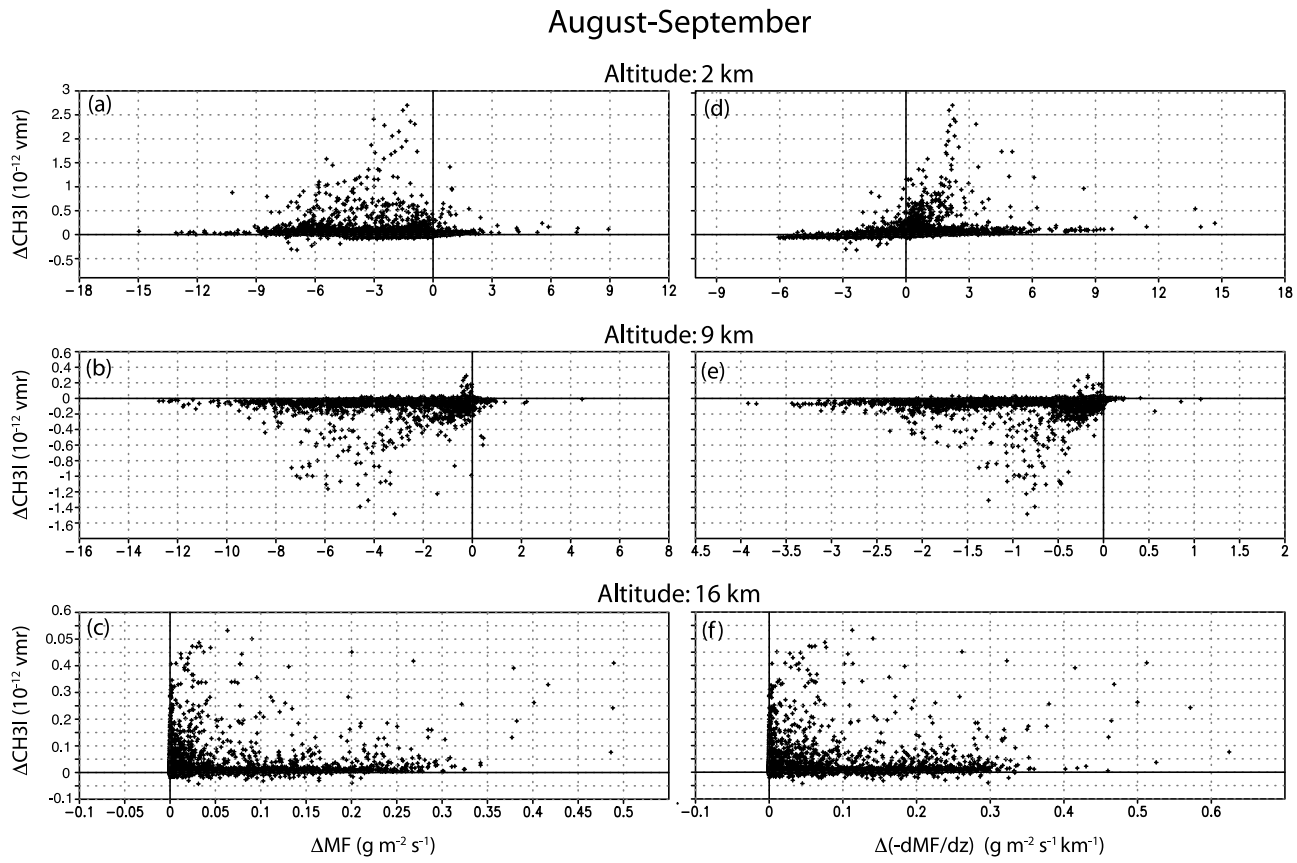

Figure 4. Differences (AM2-D minus AM2) in monthly mean methyl iodide at selected altitudes plotted against differences in monthly mean cumulus mass flux (a–c) and mass-flux convergence (d–f) (30°S to 50°N). Mass fluxes are grid-box averages, with zero flux assigned to portions of grid boxes without convection when computing averages.

lifetime of 48 h in daylight. Loss of methyl iodide by reaction with hydroxyl radicals is also included but is negligible compared to photolysis.

3. Radon and Methyl Iodide in AM2 and AM2-D

[17] Both AM2 and AM2-D are integrated for a period of 17 years (1982–1998), with results analyzed for 1983–1998. Differences in the structures of the radon and methyl iodide fields are particularly evident for the months of July and August–September, respectively, reflecting intense convection over Northern Hemisphere land during July, which produces a strong signal for radon, and a co-location of intense convection and seasonal peaks in terrestrial sources for methyl iodide in August and September.

[18] Zonal averages of the volume mixing ratio for radon (July) and methyl iodide (August–September) are shown in Figures 1 and 2, respectively. Although radon is exclusively emitted over continents, while methyl iodide has continental and marine sources, their patterns of differences between AM2-D and AM2 are similar. Chiefly, concentrations of both tracers in the middle- to upper troposphere at the latitudes of maximum concentration are greater in AM2. The altitude at which these differences are most pronounced is somewhat higher for methyl iodide than radon, and the latitude where the differences are most pronounced is closer to the Equator for methyl iodide, reflecting different emission patterns and variations in the penetrative extent of deep convection with latitude. Although concentrations of methyl iodide and radon are higher in AM2 in the middle troposphere, the concentrations in AM2-D are higher in the region around the tropopause (approximated by the temperature minimum and shown by the dots in Figures 1 and 2) in most of the tropics and northern sub-tropics. The *Donner* [1993] parameterization allows for convective cells to overshoot their levels of neutral buoyancy and transport tracers to correspondingly greater altitudes; this mechanism does not exist in the relaxed Arakawa-Schubert parameterization, which takes clouds upward only to their level of neutral buoyancy.

[19] Deep convection carrying air with boundary layer properties into the stratosphere, as in AM2-D, is consistent with the analyses of observations by *Sherwood and Dessler* [2003], *Hegglin et al.* [2004], and *Ray et al.* [2004]. The AM2 radon concentrations in the northern middle latitudes around 8 to 10 km are about 1.4 times those of AM2-D. These differences are larger than those reported by *Considine et al.* [2005] in these regions in a comparison of three chemical transport models, in which the highest values among the models were about 1.1 to 1.2 times those of the lowest values and radon concentrations were between those in AM2 and AM2-D. The concentration range noted by *Considine et al.* [2005] is due not only to differences in

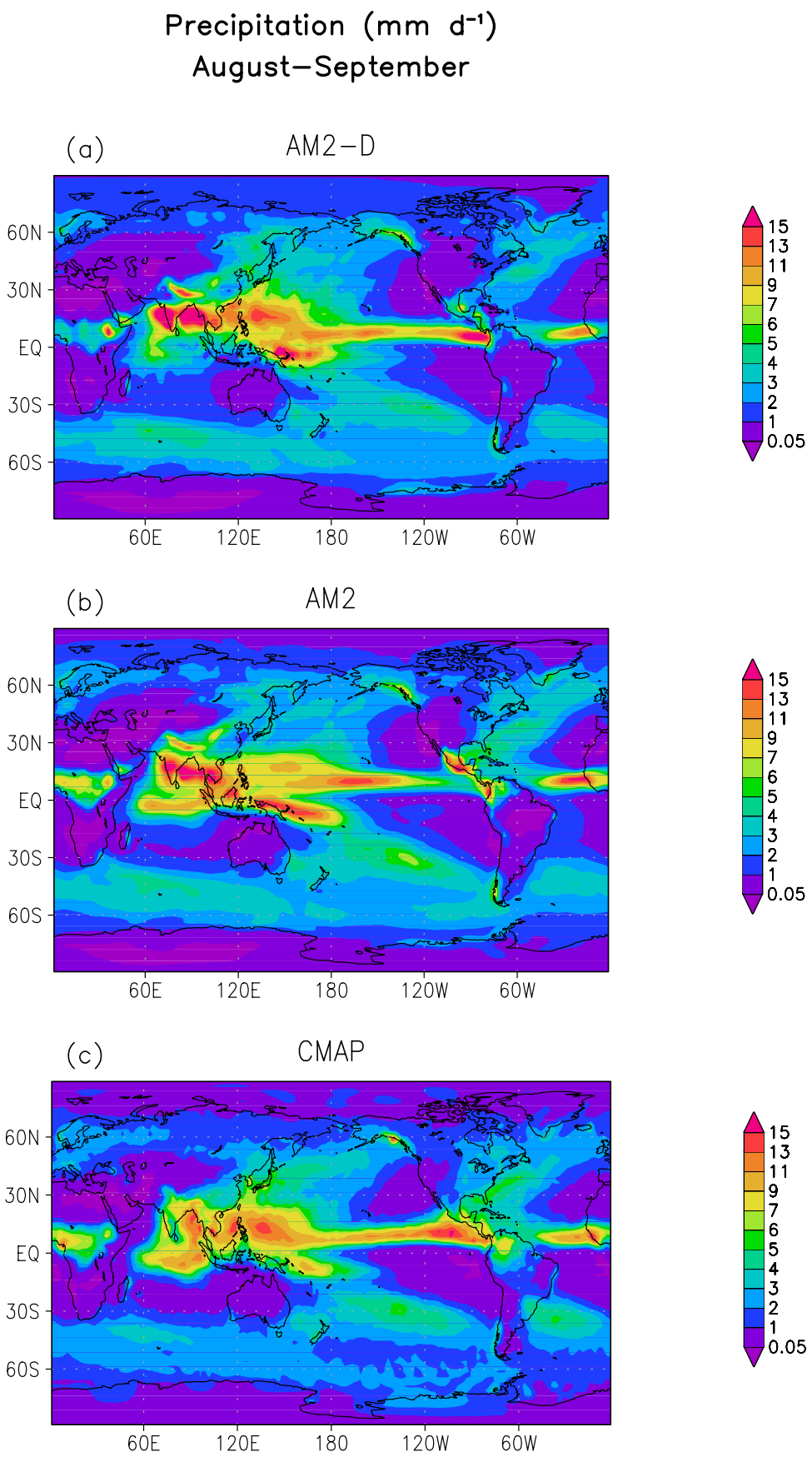

Figure 5. Total precipitation for August-September for (a) AM2-D, (b) AM2, and (c) CMAP analysis.

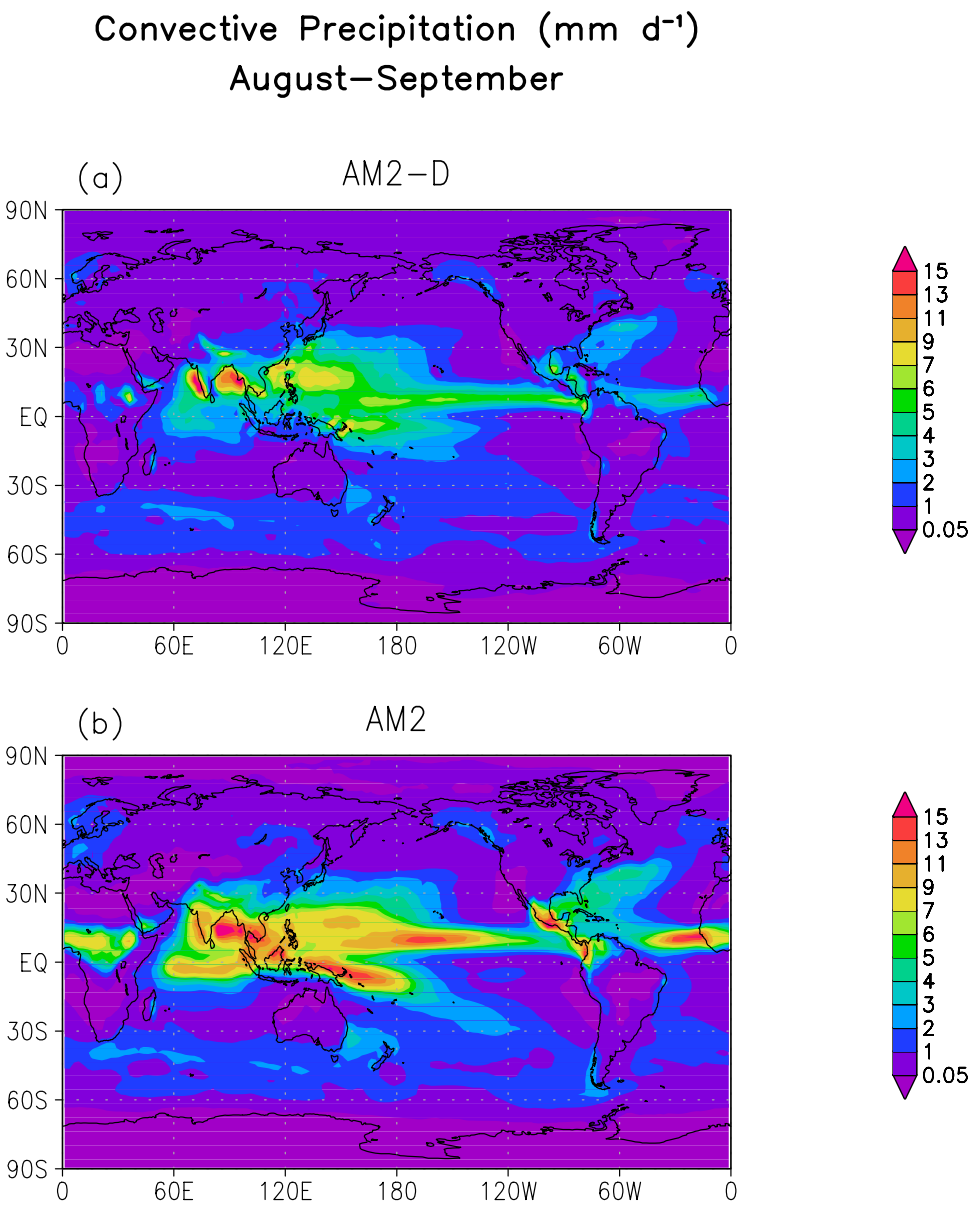

Figure 6. Convective precipitation for August–September for (a) AM2-D and (b) AM2.

cumulus parameterizations in the transport models but to differences in algorithms for advection and other physical processes as well. Their relatively small concentration range emphasizes the large degree to which the cumulus parameterizations in AM2 and AM2-D differ. Interannual variability of the zonally averaged concentrations, as measured by the standard deviations of the July (radon) and August-September (methyl iodide) means over the 1983–1998 period of the integration, is typically less than 10% of the mean values.

[20] The differences in zonally averaged concentrations of methyl iodide and radon are direct consequences of significant differences in the convective mass fluxes in AM2 and AM2-D (Figure 3). The relaxed Arakawa-Schubert cumulus parameterization employed in AM2 produces mass fluxes in the northern tropics around 8 km that are more than three times those of the *Donner* [1993] parameterization in AM2-D. The largest methyl iodide differences between AM2 and AM2-D are just south of 30°N, and the largest radon differences are between about 40 and 60°N. The latitudes with largest emissions (around 20°N for methyl iodide, 50°N for radon) differ from the latitudes with the most convection (around 10°N), but Figure 3 shows that convective mass fluxes are also greater in AM2 than AM2-D at the latitudes where concentration differences are largest. (Note that the convective mass fluxes shown for AM2-D are total mass fluxes from deep convective cells, associated mesoscale updrafts and downdrafts, and shallow convection.)

[21] These differences are larger than those reported by *Mahowald et al.* [1997] for two different transport models, one of which had maximum mass fluxes about 150% of the other. *Folkins et al.* [2006] compared mass fluxes in AM2 and AM2-D with those in four chemical transport models. They found that the three-fold difference in mass fluxes between AM2 and AM2-D bracketed the mass fluxes from

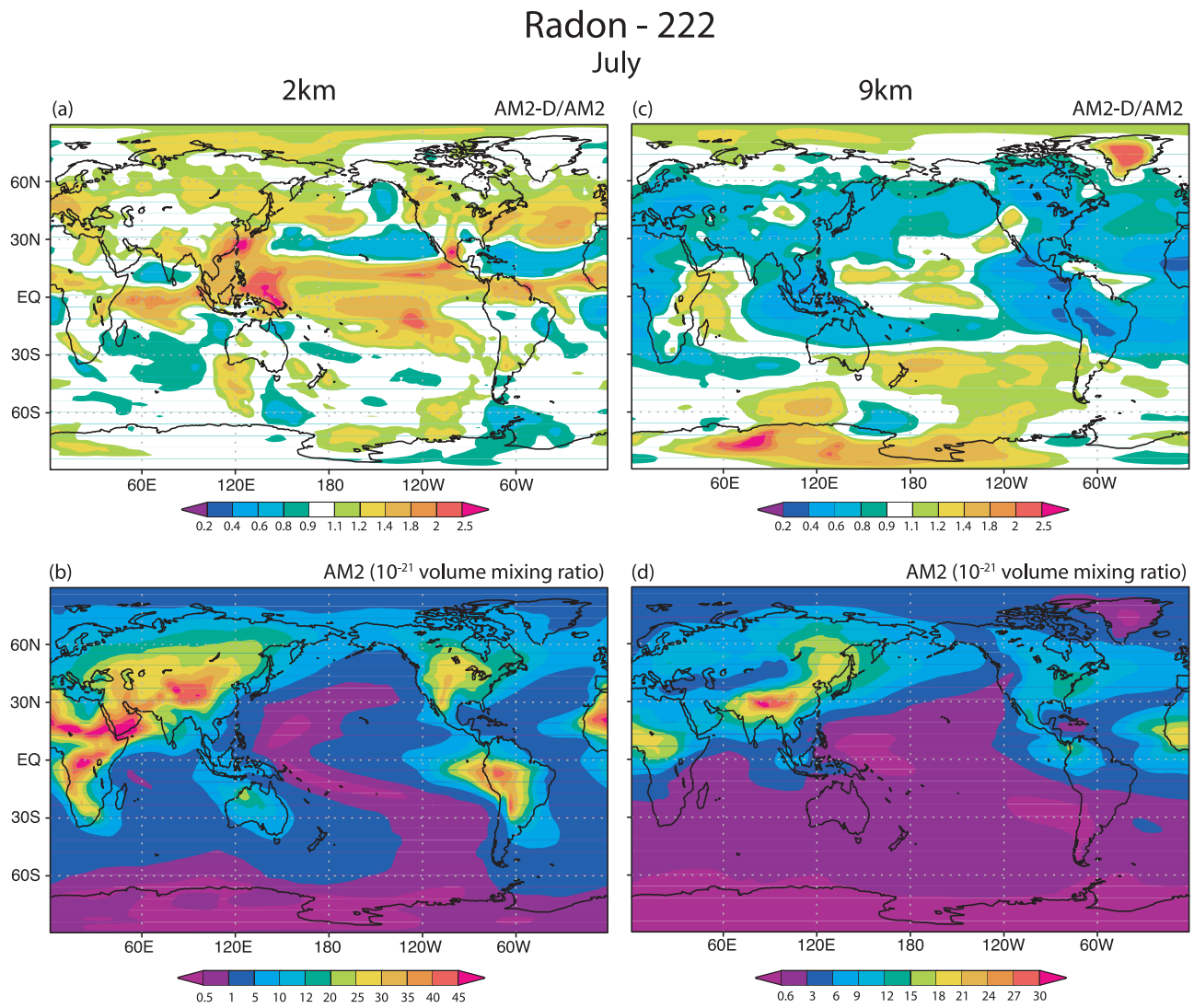

Figure 7. (a) Ratio of radon-222 concentrations in AM2-D to AM2 and (b) volume mixing ratio for AM2 at 2 km. (c) Ratio of radon-222 concentrations in AM2-D to AM2 and (d) volume mixing ratio for AM2 at 9 km.

the other models between about 6 and 8 km. It is not immediately evident which of the differing characteristics of the parameterizations are responsible for the large differences in mass fluxes (and tracer concentrations) in their study. Indeed, even the implementation details for a particular parameterization can be associated with a large range of mass fluxes. For example, in the comparison of *Folkins et al.* [2006] between 6 and 8 km, an application of the relaxed Arakawa-Schubert cumulus parameterization in a chemical transport model has mass fluxes about one-third the mass fluxes with the relaxed Arakawa-Schubert parameterization as implemented in AM2. Note that the AM2 implementation follows *GFDL Global Atmospheric Model Development Team* [2004] without modification for these comparisons with AM2-D.

[22] The larger mass fluxes at the tropopause in AM2-D are associated with larger water vapor concentrations in the tropical lower stratosphere. From 50 to 100 hPa between 30°S and 30°N, zonally averaged specific humidities are about 1.5 mg kg^{-1} larger in AM2-D. These specific humidities also depend strongly on the vertical resolution. AM2 and AM2-D both have 24 levels. The specific humidities in the tropical lower stratosphere are higher than reported from the Halogen Occultation Experiment and the Microwave Limb Sounder on the Upper Atmosphere Research Satellite [*Randel et al.*, 1998] in both AM2 and AM2-D with 24 levels. With 48 levels, AM2 is generally about 1 mg kg^{-1} too dry in the tropical lower stratosphere, while AM2-D ranges from near observed values to about 1 mg kg^{-1} too moist.

[23] Figures 4a–4c show monthly mean differences in methyl iodide concentrations (AM2-D minus AM2) plotted against monthly mean differences in mass fluxes (AM2-D minus AM2) for grid points with non-zero mass fluxes between 50°S and 30°N at 2, 9, and 16 km. At 9km, smaller mass fluxes in AM2-D are associated with smaller methyl iodide concentrations. At 16 km, larger mass fluxes in AM2-D are associated with larger methyl iodide concentrations. At 2 km, methyl iodide concentrations are larger in AM2-D, even though mass fluxes are smaller. Many cumu-

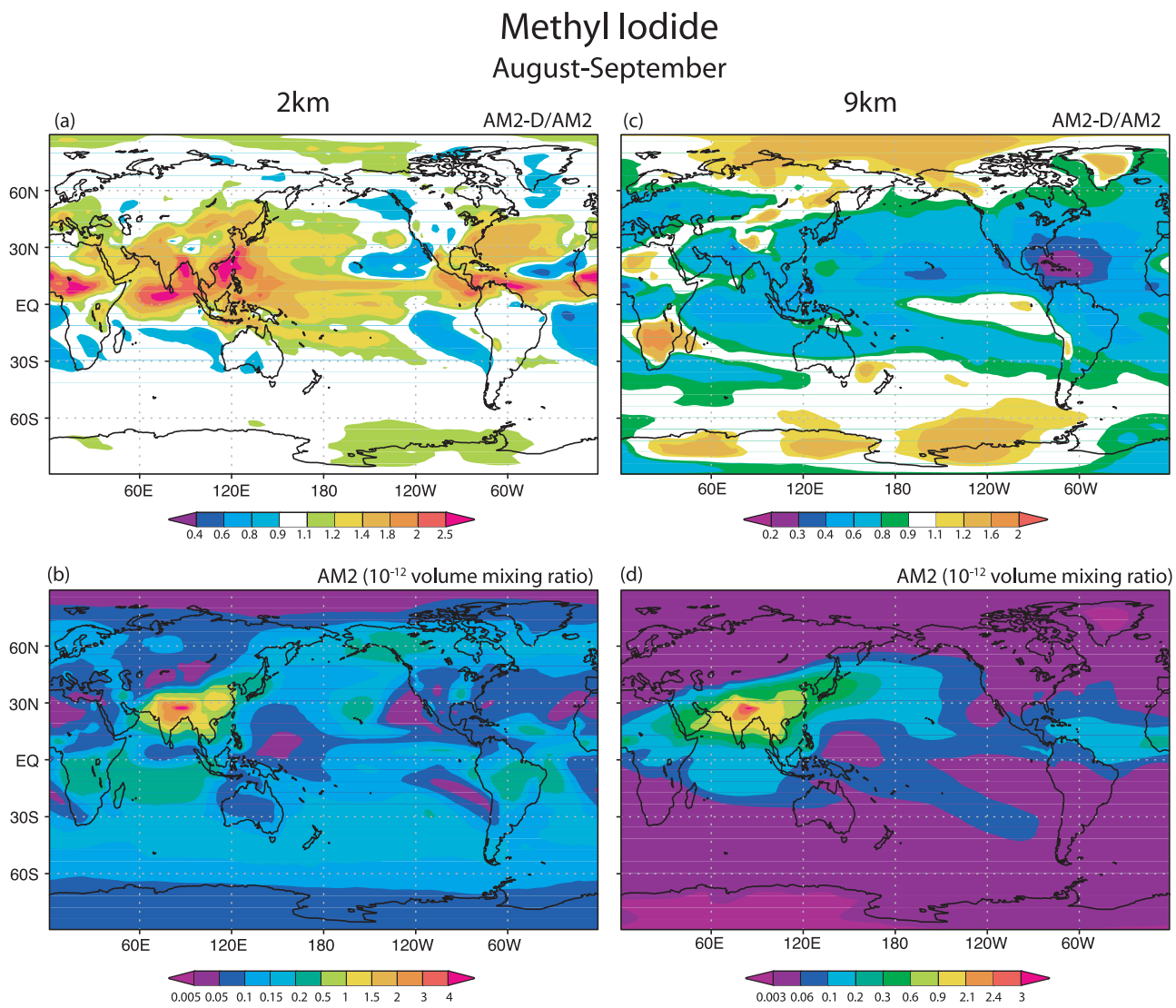

Figure 8. Same as Figure 7, except for methyl iodide.

lus cells pass through the 2-km level without detraining, so there is not a direct link there between convective mass fluxes and methyl iodide concentrations. Figures 4d–4f show the differences in the convergence of cumulus mass fluxes (detrainment). Methyl iodide concentrations vary consistently with detrainment from convection. At altitudes where detrainment is generally larger in AM2-D (2 and 16 km), methyl iodide concentrations also tend to be larger. At 9 km, where AM2-D generally has less detrainment, it also tends to have less methyl iodide. Note that emissions and advective transport can vary widely for a given mass flux or detrainment rate, so high correlation between mass fluxes or detrainment and methyl iodide concentrations is not evident.

[24] Although the connection between differences in methyl iodide and radon concentrations and profiles of convective mass flux is fairly obvious, the large differences in convective mass fluxes between AM2 and AM2-D requires further explanation. Precipitation measures the vertically integrated latent heat released by deep convection. Figure 5 shows precipitation patterns in AM2 and AM2-D, along with precipitation from CMAP (Climate Prediction Center Merged Analysis of Precipitation, described by *Xie and Arkin* [1997]). While the precipitation in the tropics and sub-tropics is similar in AM2 and AM2-D, the convective mass fluxes differ greatly. Between 30°S and 50°N, precipitation is 2% less in AM2-D than AM2, but mass fluxes are 40% less. The mass fluxes differ by over an order of magnitude more than the precipitation because AM2 and AM2-D partition precipitation between deep convection (including mesoscale anvils) and stratiform clouds very differently, as is evident in Figure 6, which shows the convective precipitation in AM2 and AM2-D. Convective precipitation is notably greater (and stratiform precipitation correspondingly less) in AM2, consistent with larger vertically integrated convective mass fluxes in AM2. The ratio of precipitation from large-scale stratiform clouds and mesoscale anvils to total precipitation in AM2-D is closer to the corresponding ratio inferred by the Tropical Rainfall Measuring Mission (TRMM) than in AM2. These ratios between 30°S to 40°N (northward limit of TRMM) are 0.46, 0.13, and 0.47 for AM2-D, AM2, and TRMM, respectively (TRMM results from http://disc.gsfc.nasa.gov/data/data-

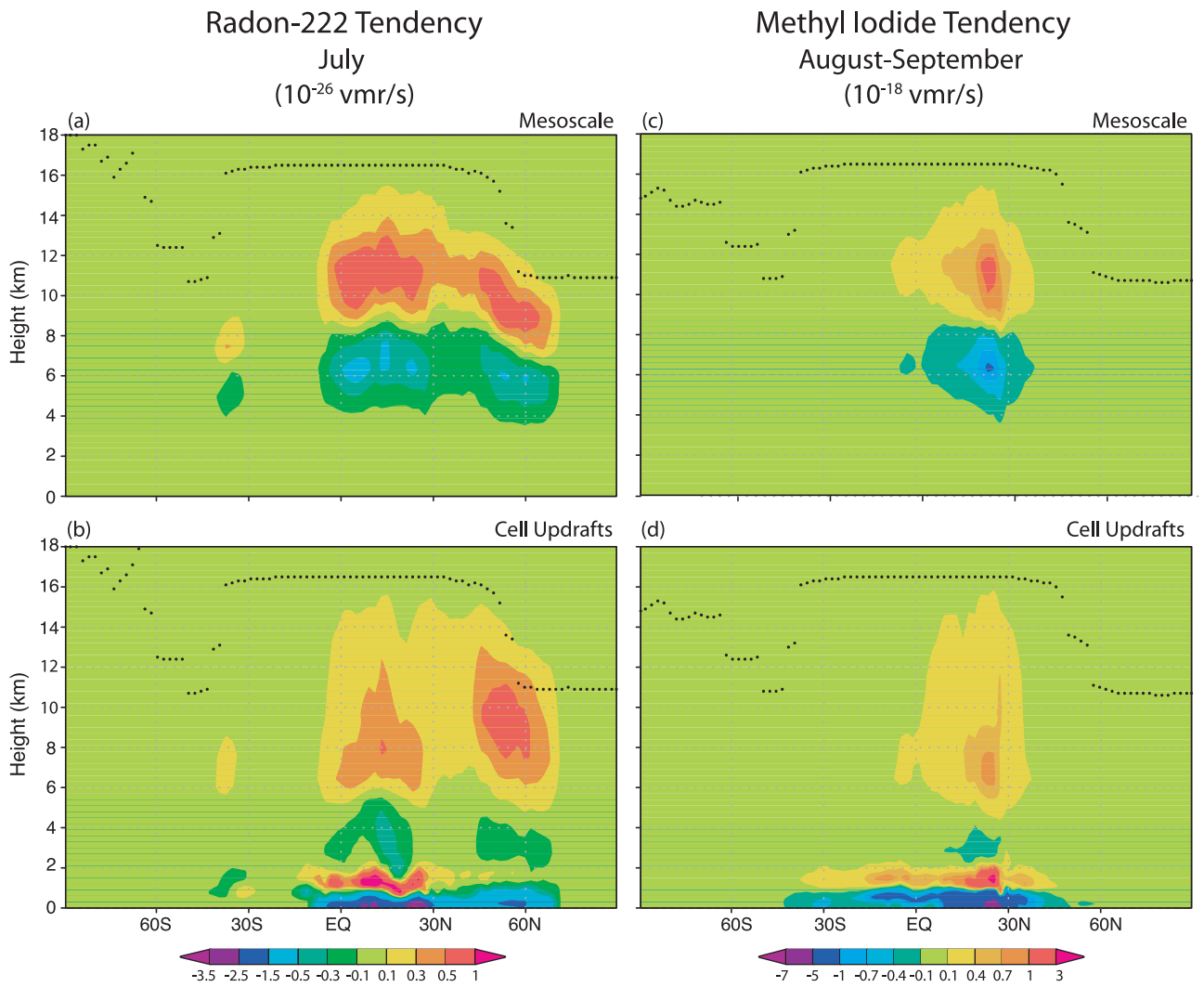

Figure 9. Radon tendency due to (a) mesoscale updrafts and (b) cell updrafts. Methyl iodide tendency due to (c) mesoscale updrafts and (d) cell updrafts. Temperature minimum (as an indication of the tropopause) indicated by dark circles.

pool/TRMM_ DP). *Donner*'s [1993] parameterization partitions more of the total convective mass flux into cumulus elements which detrain in the middle troposphere than does the relaxed Arakawa-Schubert parameterization in AM2. The more extensive mid-tropospheric detrainment of water vapor and condensate builds stratiform clouds which yield more stratiform precipitation.

[25] Soluble tracers (subject to wet deposition) would likely be removed at different rates in stratiform and convective cloud systems. Rates of removal by wet deposition depend on condensed water content and the efficiency with which a given species is removed. Condensed water contents are typically much higher in convective cells than stratiform clouds. The large differences in partitioning of convective and stratiform precipitation between AM2 and AM2-D suggest that the dependence of distributions of soluble tracers on cumulus parameterization could differ significantly from that of radon and methyl iodide.

[26] Figures 7a and 7b show the ratio of radon-222 in AM2-D to AM2 and its regional patterns at 2 km (above ground level) for AM2. The continental source of radon-222 is clearly evident at 2 km. Since radon emissions are uniform over continental regions, the concentration variability at 2 km is due to variations in the rate at which radon is transported vertically away from the surface (by advection, non-convective diffusion, and convection) and variations in horizontal advective transport. For example, some regions with high topography (Rockies, Tibetan Plateau) have colder surfaces and more overlying stability than surrounding, lower-topography regions, and radon concentrations exhibit maxima in these regions. At 2 km, radon concentrations are generally higher in AM2-D than AM2, indicative of greater convective detrainment in AM2-D in the lower troposphere. (Note in Figure 3 that AM2-D convective mass fluxes decrease more rapidly with height than in AM2). Continental radon concentrations are typically 20% to 50% higher in AM2-D than AM2 at 2 km in regions with the most convection (Figures 7a and 6). Interestingly, the largest AM2-D:AM2 ratios at 2 km occur over oceanic regions, where the radon concentrations themselves are generally smaller than over the continents. Here, the AM2-D concentrations can be over 250% of those in

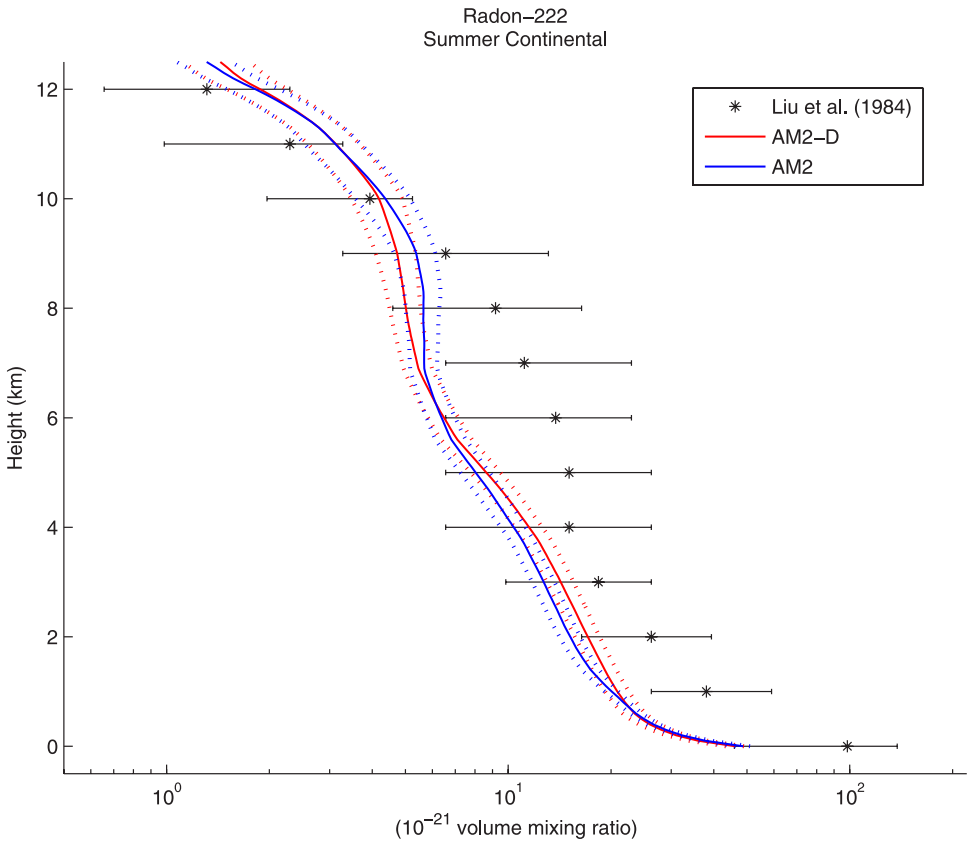

Figure 10. Vertical profile of summer continental radon volume mixing ratios from *Liu et al.* [1984], AM2, and AM2-D. Horizontal bars for *Liu et al.* [1984] indicate one standard deviation. Solid lines indicate model 1983–1998 July mean. Dotted lines indicate model 1983-1998 mean plus/minus one standard deviation of the model July means.

AM2. The patterns of these ratios reflect both long-range transport (from continental areas where radon has been convected) and local oceanic vertical transport; for example, large ratios appear in the central and eastern Pacific intertropical convergence zone (around 10°N), a region of active convection (Figure 6a), as well as in a region to the south with much less convection.

[27] Consistent with the zonal averages in Figure 1, the AM2-D:AM2 ratios are much smaller at 9 km (Figure 7c). Indeed, over most continental regions where radon is emitted, weaker vertical transport with the *Donner* [1993] parameterization results in lower radon concentrations. Extensive transport downwind of the continental sources is evident (Figure 7d). Some regions with very small radon concentrations have large ratios, for example at high latitudes. Convective precipitation over Greenland is small in both AM2 and AM2-D but is around 1.7 times heavier in AM2-D than AM2, consistent with the higher ratio at 9 km.

[28] The methyl iodide patterns at 2 km (Figure 8b) differ greatly from those of radon, reflecting emissions that are highly variable geographically with both oceanic and continental sources. The largest concentrations are over south and east Asia and result from rice production [*Bell et al.*, 2002, Table 1]. There is also a marine source of methyl iodide, which is generally about an order of magnitude smaller (per unit area) than the rice source during August and September. The marine source is larger in the subtropics and middle latitudes than in the inter-tropical convergence zone, and this pattern is also evident in the concentrations at 2 km. Large AM2-D:AM2 concentration ratios at 2 km (Figure 8a) occur mostly in regions where large methyl iodide emissions and deep convection coincide and show evidence of greater detrainment in AM2-D. Because heaviest convective precipitation coincides more closely with methyl iodide emissions than radon emissions, large ratios for radon do not coincide so closely with regions of large radon emissions (Figure 7a). AM2-D concentrations at 2 km can be more than 250% of those in AM2. The situation at 9 km is very different, with AM2-D concentrations as little as 20% to 30% of those in AM2 (Figure 8c), reflecting the lower convective mass fluxes in most regions at this altitude in AM2-D. Lower concentrations are especially evident over the Caribbean, where, in addition to differences in the vertical structure of the mass fluxes, there is also less convective precipitation in AM2-D (Figure 6). The key exception to the general pattern of low ratios at 9 km is southern Africa. Light convective precipitation falls over this region, but more heavily in AM2-D than AM2. Southern Africa is a region with a localized maximum of biomass burning, which, in conjunction with more convection in AM2-D, explains the high ratios there. A pronounced maximum in methyl iodide is evident over north India (Figures 8b, 8d), where emissions from rice cultivation exhibit a global maximum during August and Septem-

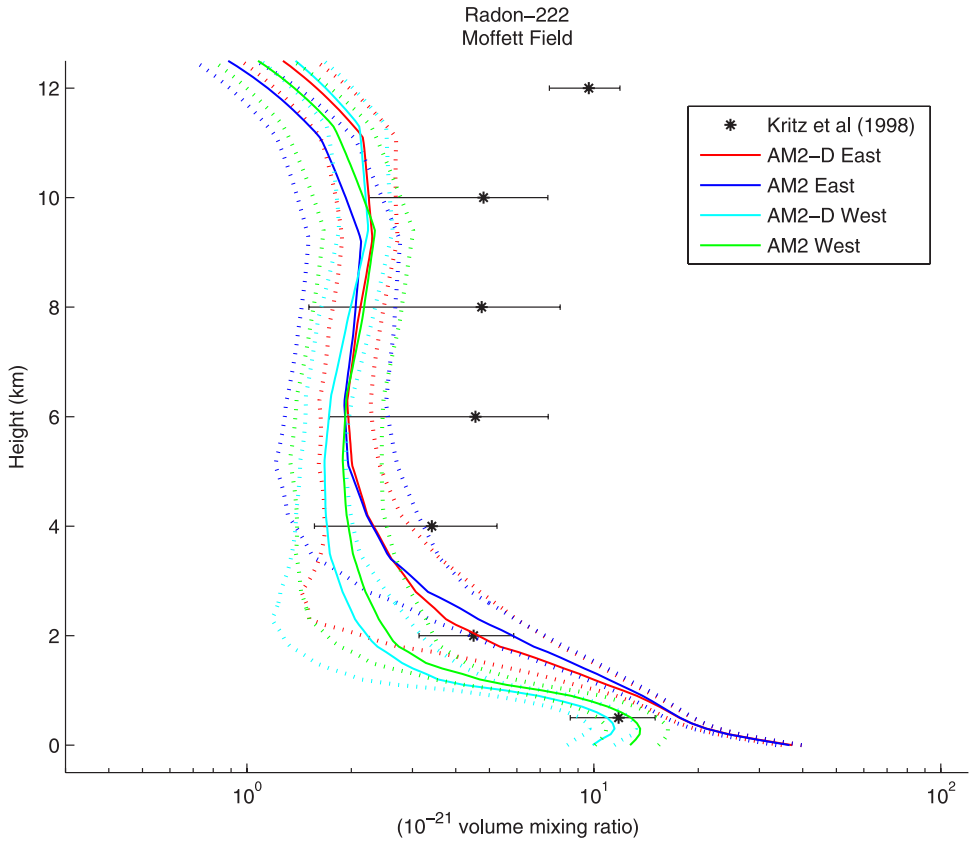

Figure 11. Vertical profile of radon observed during June 1994 at Moffett Field [*Kritz et al.*, 1998]. Profiles from AM2-D and AM2 for the model grid points west and east of Moffett Field. Horizontal bars for *Kritz et al.* [1998] show ±2 times the standard error of the averages. Solid lines indicate model 1983–1998 July mean. Dotted lines indicate model 1983–1998 mean plus/minus one standard deviation of the model July means.

ber. Figure 8d shows extensive downwind transport of methyl iodide from its source regions at 9 km.

[29] As noted in section 2, the cumulus parameterization in AM2-D includes a treatment of mesoscale circulations, while the cumulus parameterization in AM2 does not. Figure 9 shows the zonally averaged tendencies of radon and methyl iodide due to mesoscale updrafts and cell updrafts in the *Donner* [1993] parameterization. The cells exhibit a bi-modal distribution of detrainment, with shallow cumulus detraining above the PBL and over a deep layer in the middle and upper troposphere. The mesoscale circulations transport radon and methyl iodide from the middle to the upper troposphere. The rates of mesoscale removal are comparable to the rates at which cells detrain in the middle troposphere. The rates of mesoscale addition in the upper troposphere are larger than the rates at which cells add radon and methyl iodide there by detrainment. The mesoscale components of the convective systems are comparable in importance to the cell updrafts. However, note that this does not imply that cumulus parameterizations without mesoscale circulations have smaller mass fluxes or less tracer transport. Indeed, Figures 1–3 show AM2 has more radon and methyl iodide (and larger convective mass fluxes) around 10 km, where the upward mesoscale transports are large in AM2-D. The AM2 parameterization without mesoscale circulations compensates through larger mass fluxes in its deep ensemble members. As a result, detecting the signature of a mesoscale circulation solely through chemical tracer measurements in a field experiment would be difficult, although possible in conjunction with observations (e.g., by radar) of the morphology of convective systems. The effects of convective mesoscale circulations on transport are subtle and arise through enhanced upper-tropospheric heating by mesoscale and stratiform clouds. The stabilizing effects of this heating reduce mass fluxes in cell updrafts and, consequently, tracer transport.

4. GCM-Observation Comparison

[30] Observations of radon and methyl iodide are limited, generally being restricted to a few locations in space and time. Comparisons between GCM results and observations must be interpreted accordingly. In this section, model profiles are 1983–1998 time averages for July (radon) and August-September (methyl iodide), but spatial sampling is consistent with observations. Standard deviations of the model results are provided as an indication of interannual variability.

[31] Figure 10 shows the summer continental radon profile of *Liu et al.* [1984], based on 23 profiles at six locations. The heights of these individual profiles varied, with the individual profiles extending to 1 (1 profile), 2 (3

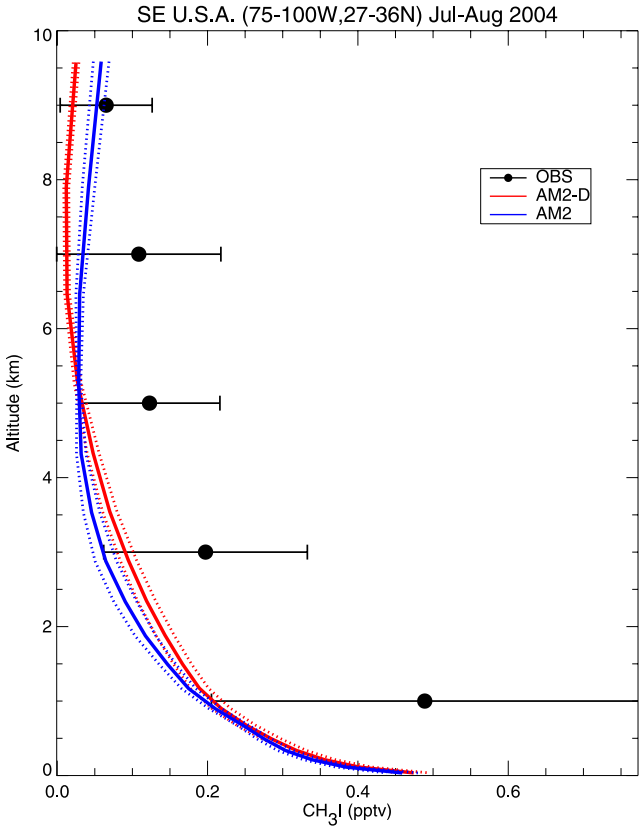

Figure 12. Vertical profiles of methyl iodide for the southeast USA from INTEX-NA field experiment, AM2-D, and AM2. Horizontal bars indicate one standard deviation calculated from individual measurements. Solid lines indicate model 1983–1998 August-September mean. Dotted lines indicate model 1983–1998 mean plus/minus one standard deviation of the model August–September means.

profiles), 4 (5 profiles), 5 (2 profiles), 8 (6 profiles), 9 (4 profiles), and 12 (2 profiles) km. The corresponding model profiles are sampled at the same locations and weighted appropriately. Both AM2 and AM2-D barely enter the low end of the observed standard deviation below 8 km, above which they move toward the high end of the observed standard deviation. The differences between AM2 and AM2-D are small compared to the differences between the observations and either of the models. AM2-D and the observations both decrease with height between 7 and 9 km, whereas AM2 is nearly constant, reflecting its larger cumulus mass fluxes in this height range (Figure 3). *Considine et al.* [2005] compared summer continental radon profiles obtained in a similar way for three chemical transport models and found more variation than between AM2 and AM2-D. As with AM2 and AM2-D, the radon concentrations in the models examined by *Considine et al.* [2005] had lower radon concentrations between 4 and 8 km than observed by *Liu et al.* [1984], and higher concentrations (in two of the three models) above 10 km. *Mahowald et al.* [1995] found a range of about a factor of two in radon concentrations in the western United States in this height range, using seven cumulus parameterizations in a column transport model, for which all but one decreased with height between 7 and 9 km. The sparseness of the observations strongly limits the extent to which they can be used to evaluate the models. Relative to the chemical transport models compared by *Considine et al.* [2005], the range of zonally averaged radon concentrations between AM2 and AM2-D is greater in the northern midlatitudes around 8 to 10 km (cf., discussion following Figure 1), but the opposite is true for observations sampled in the manner of *Liu et al.* [1984].

[32] Seven radon profiles are available from a field campaign at Moffett Field in California during June 1994 [*Kritz et al.*, 1998]. Since steep horizontal gradients might be expected between oceanic and land areas to the immediate west and east of Moffett Field, Figure 11 shows model results for the grid boxes immediately west and east, centered respectively at 123.75° and 121.25° W. (Moffett Field is at 122.0° W.) Here, observations show a considerably more "C-shaped" profile than the summer continental average of *Liu et al.* [1984]. Although neither AM2 nor AM2-D captures the full extent of the upper-tropospheric maximum, AM2-D shows more "C-shape" than AM2. As for the summer continental profiles, *Considine et al.*'s [2005] Moffett profiles show more spread than AM2 and AM2-D, with the chemical transport models exhibiting an order of magnitude range in radon at 12 km. As for AM2 and AM2-D, all of the model profiles in *Considine et al.* [2005] show less radon than is observed above 4 km. In summary, while both AM2 and AM2-D depart in similar ways from radon observations, AM2-D is somewhat more successful than AM2 in simulating both the decrease of radon with height in the middle troposphere in the summer continental mean and the increase of radon with height in the upper troposphere in the Moffett Field observations.

[33] Currently available radon observations allow few inferences about AM2, AM2-D, and the chemical transport models discussed above. The differences between AM2-D and AM2 are small relative to the other models for Moffett Field and sites in *Liu et al.* [1984], but zonally averaged differences between AM2-D and AM2 are larger than in the regions from which observations are available, illustrating that observations are not yet sufficiently dense to be representative of global patterns. Even if globally representative observations were available, it would be important to recognize that the differences between models and parameterizations represent aggregate effects of different cumulus parameterizations, parameterizations of other physical processes, and numerical algorithms. A useful future observational strategy would be to obtain tracer budgets in regions of deep convection, including advective transports into the region of convection. From these observations and the time evolution of tracer concentrations, the convective component of tracer transport could be isolated. This strategy has been used to obtain observed diagnoses of heat and moisture sources due to convection [cf. Figure 6 of *Donner*, 1993].

[34] Measured (on the NASA DC-8 aircraft during the summer 2004 INTEX-NA field campaign) and modeled methyl iodide in the southeast USA show behavior similar to summer continental radon (Figure 12). Both AM2 and AM2-D underestimate observed methyl iodide values from the top of planetary boundary layer through most of the

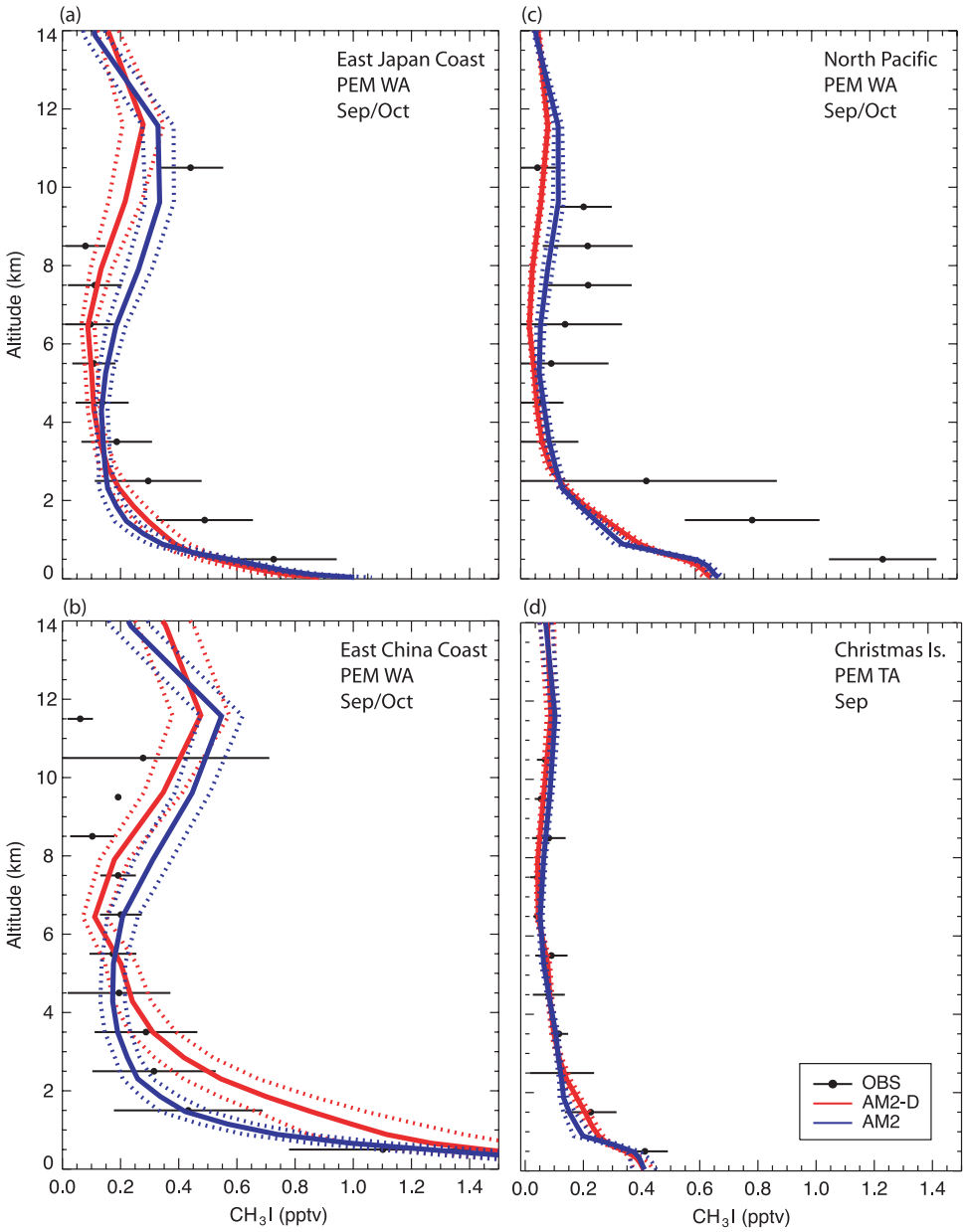

Figure 13. Observed vertical profiles of methyl iodide from *Bell et al.* [2002] and profiles from AM2-D and AM2 for (a) east Japan coast, (b) east China coast, (c) north Pacific, and (d) Christmas Island. Horizontal bars are standard deviations calculated from individual measurements. In (b), there is only one observation at 9.5 km. Solid lines indicate model 1983–1998 August-September mean. Dotted lines indicate model 1983–1998 mean plus/minus one standard deviation of the model.

troposphere. AM2 exhibits a "C-shaped" profile not evident in the observations or AM2-D, a result again consistent with AM2-D's smaller cumulus mass fluxes in the middle-to-upper troposphere.

[35] *Bell et al.* [2002] compiled observed profiles for methyl iodide over marine regions from several field campaigns. Figure 13 shows four of these profiles during the September-October time period along with profiles from AM2 and AM2-D. In all cases, the profiles of AM2 are more "C-shaped" than those of AM2-D. For the east China coast and Christmas Island, AM2-D's profiles match observations more closely in this regard. The north Pacific observations are more "C-shaped" than either AM2 or AM2-D, and in this case AM2 is more realistic. Interannual variability of methyl iodide, as measured by standard deviations of August-September means, varies regionally and can be a larger fraction of mean values than was evident in the zonal means (Figures 1, 2). Spread among the observations is generally large compared to interannual variability in the model means.

[36] *Bell et al.* [2002] also calculated a "convective index" for methyl iodide, the ratio of concentrations in the layers between 8–12 km and 0–2.5 km. Table 1 shows her observed and modeled indices, along with those of AM2 and AM2-D, roughly corresponding to the months analyzed in this paper. AM2-D's convective indices are generally

Table 1. Methyl Iodide Convective Index[a]

REGION	*Bell et al.* [2002] *Observed*	*Bell et al.* [2002] *Simulated*	AM2-D	AM2
North Pacific 180–150°W, 15–35°N Sept.–Oct. 1991	0.22	0.41	0.21 (.03)	0.37 (.07)
Hawaii 170–150°W, 10–30°N Sept. 1996	0.20	0.39	0.19 (.03)	0.38 (.08)
Christmas Island 160–140°W, 0–10°N Sept. 1996	0.24	0.37	0.28 (.04)	0.43 (.08)
Fiji 170°E–170°W, 10–30°S Sept. 1996	0.16	0.14	0.18 (.02)	0.25 (.05)
Tahiti 160–130°W, 0–20°S Sept. 1996	0.23	0.19	0.21 (.02)	0.26 (.03)

[a]Dates apply to field campaigns; model results are multi-year averages. Standard deviations of August–September model convective indices indicated in parentheses.

close to those observed by *Bell et al.* [2002], while the AM2 values show considerably more transport to the upper troposphere. The observed methyl iodide behavior is consistent with lower cumulus mass fluxes in AM2-D.

[37] Observations of both radon, with a continental source, and methyl iodide, with both marine and localized continental sources, suggest that cumulus mass fluxes in AM2 are excessive in the middle and upper troposphere. AM2-D has lower convective mass fluxes, and the associated radon and methyl iodide profiles agree more closely with observed values.

5. Summary

[38] Distributions of two chemical tracers with different regional sources have been examined with particular attention to the role of parameterized deep convection in their transport. Radon-222 is emitted over continental areas, and methyl iodide has a marine source, as well as continental sources in regions of rice production, wetlands, and biomass burning. The study emphasized late northern hemisphere summer, when continental convection occurs frequently. Two approaches to parameterizing ensembles of deep convection were used. In AM2, the convective system consists solely of an ensemble of deep cells whose intensities depend on the rate at which their cloud work function relaxes to a threshold value. In AM2-D, the convective system consists of an ensemble of cells whose relative frequencies are chosen to produce an observationally plausible distribution of vertical velocities, augmented by a mesoscale circulation.

[39] Concentrations of both radon and methyl iodide are lower in the middle- to upper troposphere in AM2-D, consistent with lower cumulus mass fluxes in AM2-D in the middle- to upper troposphere. The lower mass fluxes in AM2-D are related to a larger fraction of its precipitation falling from stratiform clouds; total precipitation is similar in both AM2-D and AM2. The larger fractional rates of stratiform precipitation in AM2-D are more consistent with satellite observations of precipitation. Observed shapes of the vertical profiles of both radon and methyl iodide are also more consistent with the lower cumulus mass fluxes in AM2-D.

[40] In the tropopause regions in both the tropics and northern middle latitudes, concentrations of both radon and methyl iodide are higher in AM2-D, opposite the behavior in the middle- to upper troposphere. This difference results from the ability of cumulus cells in AM2-D to overshoot their level of zero buoyancy, a consequence of determining their cloud tops by a vertical momentum equation (instead of neutral buoyancy, used in AM2).

[41] Given the precipitation differences between AM2 and AM2-D, which are small relative to the large differences in cumulus mass fluxes, these results show the important role that chemical tracers can play in evaluating cumulus parameterizations. The large differences in tracer distributions between AM2 and AM2-D indicate the importance of improving cumulus parameterizations in models used to study chemical transport. The infrequent spatial and temporal sampling of these tracers remains a limitation which can be lessened by future measurements of these tracers in field campaigns. Also, the presence of similar errors in tracer distributions in both AM2 and AM2-D points to the need for further development of both cumulus parameterizations and other transport-controlling physical parameterizations and numerics, e.g., planetary boundary layer. Emission sources may also require further refinement. Future experiments with aerosol tracers (e.g., lead-210, beryllium-7) and soluble gases (e.g., nitric acid) can provide additional constraints on transport and wet removal of tracers by cumulus convection.

Appendix A: Deep Cumulus Parameterizations in AM2 and AM2-D

Triggers

AM2 Cloud work function exceeds threshold depending on updraft depth.

AM2-D 1) Positive CAPE.
2) Positive CAPE tendency due to non-convective processes above PBL.
3) Convective inhibition less than threshold (100 J kg^{-1}).
4) Time-integrated low-level ascent sufficient to lift parcels to level of free convection.
5) Pressure at level of zero buoyancy is at least 500 hPa less than pressure at level of free convection.

Convective Morphology

AM2 1) Entraining updraft cells with precipitation taken as a fraction of condensed water dependent on updraft detrainment level.
2) Evaporation of precipitation.
3) Deep updraft cells allowed only if lateral entrainment exceeds lower bound.

AM2-D 1) Phase changes and transports in entraining updraft cells, mesoscale updrafts, mesoscale downdrafts, cell-scale downdrafts.
2) Vertical velocities and single-moment microphysics in updraft cells.

Closures

AM2 Mass fluxes related to rate at which cloud work function relaxes to threshold. Relaxation timescale is function of updraft depth.

AM2-D 1) Precipitation such that CAPE reduction by convective system balances CAPE generation by non-convective processes above PBL.
2) Mass flux partitioned among cell updrafts based on probability distribution function for convective vertical velocities.
3) Detrainment from updraft cells and mesoscale updraft dynamics determine mesoscale condensation.

[42] **Acknowledgments.** We thank David Considine (NASA) for providing the Moffett radon profiles, Dale Allen (University of Maryland) for providing the continental radon profiles, and Nadine Bell for providing methyl iodide emissions, observations, and processing codes. Cyril Crevoisier (Princeton University) and Song-Miao Fan (GFDL) provided helpful reviews of an early version of the manuscript, as did our anonymous reviewers.

References

Allen, D. J., R. B. Rood, A. M. Thompson, and R. D. Hudson (1996), Three-dimensional radon 222 calculations using assimilated meteorological data and a convective mixing algorithm, *J. Geophys. Res.*, *101*, 6871–6881.

Allen, D. J., K. E. Pickering, and A. Molod (1997), An evaluation of deep convective mixing in the Goddard Chemical Transport Model using International Satellite Cloud Climatology Project cloud parameters, *J. Geophys. Res.*, *102*, 25,467–25,476.

Arakawa, A., and W. H. Schubert (1974), Interaction of a cumulus cloud ensemble with the large-scale environment: Part 1., *J. Atmos. Sci.*, *31*, 674–701.

Bell, N., L. Hsu, D. J. Jacob, M. G. Schultz, D. R. Blake, J. H. Butler, D. B. King, J. M. Lobert, and E. Maier-Reimer (2002), Methyl iodide: Atmospheric budget and use as a tracer of marine convection in global models, *J. Geophys. Res.*, *107*(D17), 4340, doi:10.1029/2001JD001151.

Chevillard, A., P. Ciais, U. Karstens, M. Heimann, M. Schmidt, I. Levin, D. Jacob, R. Podzun, V. Kazan, H. Sortorius, and E. Weingartner (2002), Transport of 222Rn using the regional model REMO: A detailed comparison with measurements over Europe, *Tellus*, *54B*, 850–871.

Cohan, D. S., M. G. Schultz, D. J. Jacob, B. G. Heikes, and D. R. Blake (1999), Convective injection and photochemical decay of peroxides in the tropical upper troposphere: methyl iodide as a tracer of marine convection, *J. Geophys. Res.*, *104*, 5717–5724.

Considine, D. B., D. J. Bergmann, and H. Liu (2005), Sensitivity of Global Modeling Initiative chemistry and transport model simulations of radon-222 and lead-210 to input meteorological data, *Atmos. Chem. Phys.*, *5*, 3389–3406.

Delworth, T. D., et al. (2006), GFDL's CM2 global coupled climate models-Part I: Formulation and simulation characteristics, *J. Climate*, *19*, 643–674.

Dentener, F., J. Feichter, and A. Jeuken (1999), Simulation of the transport of Rn^{222} using on-line and off-line global models at different horizontal resolutions: A detailed comparison with measurements, *Tellus*, *51B*, 573–602.

Donner, L. J. (1993), A cumulus parameterization including mass fluxes, vertical momentum dynamics, and mesoscale effects, *J. Atmos. Sci.*, *50*, 889–906.

Donner, L. J., C. J. Seman, and R. S. Hemler (2001), A cumulus parameterization including mass fluxes, convective vertical velocities, and mesoscale effects: Thermodynamic and hydrological aspects in a general circulation model, *J. Climate*, *14*, 3444–3463.

Feichter, J., and P. J. Crutzen (1990), Parameterization of vertical tracer transport due to deep cumulus convection in a global transport model and its evaluation with ^{222}Radon measurements, *Tellus*, *42B*, 110–117.

Folkins, I., P. Bernath, C. Boone, L. J. Donner, A. Eldering, G. Lesins, R. V. Martin, B.-M. Sinnhuber, and K. Walker (2006), Testing convective parameterizations with tropical measurements of HNO_3, CO, H_2O, and O_3: Implications for the water vapor budget, *J. Geophys. Res.*, *112*, D23304, doi:10.1029/2006JD007325.

Geophysical Fluid Dynamics Laboratory Global Atmospheric Model Development Team (2004), The GFDL new global atmosphere and land model AM2/LM2: Evaluation with prescribed SST simulations, *J. Climate*, *17*, 4641–4673.

Gidel, L. T. (1983), Cumulus cloud transport of transient tracers, *J. Geophys. Res.*, *88*, 6587–6599.

Gilliland, A. B., and D. E. Hartley (1998), Interhemispheric transport and the role of convective parameterizations, *J. Geophys. Res.*, *103*, 22,039–22,045.

Gray, S. L. (2003), A case study of stratosphere to troposphere transport: The role of convective transport and the sensitivity to model resolution, *J. Geophys. Res.*, *108*(D18), 4590, doi:10.1029/2002JD003317.

Hegglin, M. I., et al. (2004), Tracing troposphere-to-stratosphere transport above a mid-latitude deep convective system, *Atmos. Chem. Phys.*, *4*, 741–756.

Jacob, D. J., et al. (1997), Evaluation and intercomparison of global atmospheric transport models using ^{222}Rn and other short-lived tracers, *J. Geophys. Res.*, *102*(D5), 5953–5970.

Josse, B., P. Simon, and V.-H. Peuch (2004), Radon global simulations with the multiscale chemistry and transport model MOCAGE, *Tellus*, *56B*, 339–356.

Kritz, M. A., S. W. Rosner, and D. Z. Stockwell (1998), Validation of an off-line three-dimensional chemical transport model using observed radon profiles. I. Observations, *J. Geophys. Res.*, *103*, 8425–8432.

Li, Y., and J. S. Chang (1996), A three dimensional global episodic tracer transport model. 1: Evaluation of its transport processes by radon222 simulations, *J. Geophys. Res.*, *101*, 25,931–25,947.

Lin, S.-J. (2004), A "vertically Lagrangian" finite-volume dynamical core for global models, *Mon. Wea. Rev.*, *132*, 2293–2307.

Lintner, B. R., A. B. Gilliland, and I. Y. Fung (2004), Mechanisms of convection-induced modulation of passive tracer interhemispheric transport interannual variability, *J. Geophys. Res.*, *109*(D13), D13102, doi:10.1029/2003JD004306.

Liu, S. C., J. R. McAfee, and R. J. Cicerone (1984), Radon 222 and tropospheric vertical transport, *J. Geophys. Res.*, *89*, 7291–7297.

Liu, H., D. J. Jacob, I. Bey, and R. M. Yantosca (2001), Constraints from ^{210}Pb and ^{7}Be on wet deposition and transport in a global three-dimensional chemical tracer model driven by assimilated meteorological fields, *J. Geophys. Res.*, *106*, 12,109–12,128.

Lu, R., C. Lin, R. Turco, and A. Arakawa (2000), Cumulus transport of chemical tracers. Part 1: Cloud-resolving model simulations, *J. Geophys. Res.*, *105*, 10,001–10,021.

Mahowald, N., P. J. Rasch, and R. G. Prinn (1995), Cumulus parameterizations in chemical transport models, *J. Geophys. Res.*, *100*, 26,173–26,190.

Mahowald, N. M., P. J. Rasch, B. E. Eaton, S. Whittlestone, and R. G. Prinn (1997), Transport of ^{222}radon to the remote troposphere using the model of atmospheric transport and chemistry and assimilated winds from ECMWF and the National Center for Environmental Prediction/NCAR, *J. Geophys. Res.*, *102*, 28,139–28,151.

Moorthi, S., and M. J. Suarez (1992), Relaxed Arakawa-Schubert: A parameterization of moist convection for general circulation models, *Mon. Wea. Rev.*, *120*, 978–1002.

Mullendore, G. L., D. R. Durran, and J. R. Holton (2005), Cross-tropopause transport in midlatitude convection, *J. Geophys. Res.*, *110*, D06113, doi:10.1029/2004JD005059.

Olivie, D. J. L., P. F. J. Velthoven, A. C. M. Beljaars, and H. M. Kelder (2004), Comparison between archived and off-line diagnosed convective mass fluxes in the chemistry transport model TM3, *J. Geophys. Res.*, *109*(D11), D11303, doi:10.1029/2003JD004036.

Ray, E. A., et al. (2004), Evidence of the effect of summertime midlatitude convection on the subtropical lower stratosphere from CRYSTAL-FACE tracer measurements, *J. Geophys. Res.*, *109*(D18), D18304, doi:10.1029/2004JD004655.

Randel, W. J., F. Wu, J. M. Russell III, A. Roche, and J. W. Waters (1998), Seasonal cycles and QBO variations in stratospheric CH_4 and H_2O observed in UARS HALOE data, *J. Atmos. Sci.*, *55*, 163–185.

Ridley, B., et al. (2004), Convective transport of reactive constituents to the tropical and mid-latitude tropopause region: I. Observations, *Atmos. Environ.*, *38*, 1259–1274.

Sherwood, S. C., and A. E. Dessler (2003), Convective mixing near the tropical tropopause: Insights from seasonal variations, *J. Atmos. Sci.*, *60*, 2674–2685.

Stockwell, D. Z., and M. P. Chipperfield (1999), A tropospheric chemical-transport model: Development and validation of the model transport schemes, *Q. J. R. Meteorol. Soc.*, *125*, 1747–1783.

Stockwell, D. Z., M. A. Kritz, M. P. Chipperfield, and J. A. Pyle (1998), Validation of an off-line three-dimensional chemical transport model using observed radon profiles. Part 2: Model results, *J. Geophys. Res.*, *103*, 8433–8445.

Wilcox, E. M., and L. J. Donner (2007), The frequency of extreme rain events in satellite observations and an atmospheric general circulation model, *J. Climate*, *20*, 53–69, doi:10.1175/JCLI3987.1.

Xie, P., and P. A. Arkin (1997), Global precipitation: A 17-year monthly analysis based on gauge observations, satellite estimates, and numerical model outputs, *Bull. Am. Meteorol. Soc.*, *78*, 2539–2558.

Zhang, G. (2002), Convective quasi-equilibrium in midlatitude continental environment and its effect on convective parameterization, *J. Geophys. Res.*, *107*(D14), 4220, doi:10.1029/2001JD001005.

Zhang, G. J. (2003), Convective quasi-equilibrium in the tropical western Pacific: Comparison with midlatitude continental environment, *J. Geophys. Res.*, *108*(D19), 4592, doi:10.1029/2003JD003520.

D. R. Blake and N. J. Blake, University of California, Irvine, CA, USA.

L. J. Donner, A. M. Fiore, L. W. Horowitz, and C. J. Seman, Geophysical Fluid Dynamics Laboratory/NOAA, Princeton University, Forrestal Campus, 201 Forrestal Rd., Princeton, NJ 08540, USA. (leo.j.donner@noaa.gov)